

THE PERFORMANCE OF SOLID-ELECTROLYTE CELLS AND BATTERIES
ON CO-H₂ MIXTURES; A 100-WATT SOLID-ELECTROLYTE
POWER SUPPLY*

D. H. Archer, L. Elikan, and R. L. Zahradnik

Westinghouse Research Laboratories
Beulah Road, Churchill Borough
Pittsburgh 35, Pennsylvania

INTRODUCTION

Fuel cells employing a ZrO₂-based electrolyte are customarily operated at temperatures around 1000°C in order to promote high oxygen ion conductivity in this solid, ceramic material. At such high temperatures commercial fuels - coal and hydrocarbons - are thermodynamically unstable; they tend to crack forming solid carbon and hydrogen gas. The deposition of carbon in solid-electrolyte batteries can be prevented by mixing with the incoming fuel a portion of the CO₂ and H₂O products emerging from the battery. These gases reform the fuel producing CO and H₂ which are then oxidized in the solid-electrolyte cells to produce power. Essentially, therefore, in utilizing commercial fuels solid-electrolyte cells operate on CO-H₂ mixtures.

Experiments have been performed to characterize the performance of solid-electrolyte cells on fuel gas mixtures containing CO, H₂, CO₂, and H₂O in various proportions. Open circuit voltages have been determined in single cells at various temperatures; the measured values of voltage agree with those computed from thermodynamic data within 3%. The dependence of the operating voltage of solid-electrolyte cells on the current drain (or current density) has also been studied at various temperatures for different fuel mixtures. In general, cells operating on CO-CO₂ mixtures develop less output voltage than those operating on H₂-H₂O because of increased polarization voltage losses. The addition of H₂-H₂O to CO-CO₂ mixtures, however, greatly reduces these losses. And the insertion of a catalyst into the cell which promotes the shift reaction



causes further reduction in the observed polarizations to the extent that cell performance on CO-H₂ fuel duplicates that on pure H₂.

Tubular, solid-electrolyte batteries containing 20 bell-and-spigot cells of 7/16 in. diameter and 7/16 in. length have been produced. They are leak-tight. Their resistance has been

*The work recorded in this paper has been carried out under the sponsorship of the Office of Coal Research, U.S. Department of the Interior, and Westinghouse Research Laboratories. Mr. George Fumich, Jr., is head of O.C.R.; Neal P. Cochran, Director of Utilization, and Paul Towson have monitored the work for O.C.R.

of oxygen to gm-atoms of carbon in the fuel gas mixture - and n_H^1 , a similar ratio for hydrogen and carbon. Experimental values of open-circuit voltage are plotted together with theoretical curves in Figures 2 and 3. Except at $n_O = 1.0$ (usually corresponding to pure CO) and $n_O = 2.0$, $n_H^1 = 0.0$ (pure CO₂) where E_t changes very rapidly with n_O , E_t values are within $\pm 3\%$ of the predicted values. This agreement is considered to be within the limits of accuracy of the measurements of composition, temperature, and voltage involved.

VOLTAGE-CURRENT RELATIONS

The single solid-electrolyte cell shown in Figure 1 was also used to determine voltage-current curves for various mixtures of CO, H₂, CO₂, and H₂O at different temperatures. Some of the experimental results are shown in Figures 4-7.

When a current is drawn from the terminals, the voltage of the cell drops below the open-circuit voltage because of resistance losses in the electrolyte and electrodes and because of polarization voltage losses associated with irreversible electrode process.

$$V = E_t - IR - V_p \quad (2)$$

where V = the terminal voltage of the cell, volts

E_t = the open circuit voltage of the cell (which can be determined from Figures 2 or 3), volts

I = the load current passing through the cell, amperes

R = the electrical resistance of electrodes and electrolyte, ohms

V_p = the polarization voltage loss, volts.

An approximate value for the resistance of the cell shown in Figure 1 can be computed from

$$R = \rho_b \delta_b / A_b + (\rho_e / \delta_e)(L_e / P_e) \quad (3)$$

where ρ_b = electrolyte resistivity, about 70 ohm-cm at 1000°C

δ_b = electrolyte thickness, 0.09 cm

A_b = active cell area, 27.6 cm²

ρ_e / δ_e = resistivity-thickness quotient for the cell electrodes, estimated to be 0.8 ohms

L_e = mean distance traveled by the electronic current in the electrodes passing from the plus to the minus terminal of the cell, estimated to be 4 cm

P_e = mean width of the electrode perpendicular to the direction of electronic current flow, calculated as 3.4 cm

$$\begin{aligned} R &= [(70)(0.09)/27.6] + [(0.8)(4/3.4)] \\ &= 0.23 \text{ ohms} + 0.94 \text{ ohms} \\ &= 1.2 \text{ ohms.} \end{aligned}$$

The cell resistance has also been determined by measuring the voltage loss over the cell while passing a current with air at both inner and outer electrodes. The constant slope of this curve at higher current densities is termed the air-air resistance. Generally, this resistance value checks the resistance as computed above. Immediately after its construction the air-air resistance of the cell of Figure 1 checked the calculated resistance. Before the data for Figures 4-7 were obtained - three months later, the electrolyte component of cell resistance had gradually doubled. Presumably, the active cell area had decreased to about one-half the superficial electrode area.

Values of the polarization voltage V_p have been computed by Equation 2 from data of the type presented in Figures 4-7. For these computations the air-air resistance values were used, and E_t values were corrected by the use of Figures 2 and 3 where the cell current produced any appreciable change in n_0 , the oxygen content of the fuel stream passing through the cell. Table 1 presents the V_p values and also gives derived values of αn and i_0 in the simplified Tafel equation³

$$V_p = \frac{RT}{\alpha n} [\ln(i/i_0)] \quad (4)$$

where α is an empirically determined fraction of the electrical work output by which the free energy of activation is increased. An α value of about 0.5 is usually assumed in cases where specific knowledge is lacking.

n is the number of electrons transferred for each occurrence of the irreversible event causing the polarization voltage loss; n is assumed to be 2 in the electrochemical oxidation of CO.

i is the current density I/A_p , amperes/cm².

i_0 is the exchange current density, the equal but opposite rates at which the polarization-causing process and its reverse occur at open circuit (assuming a reversible electrode at this condition).

The following general observations can be made based on the data for pure, dry CO-CO₂ fuel mixtures presented in Figures 4-6 and Table 1:

- 1) Polarization losses in solid-electrolyte cells with conventional electrodes are much greater than those observed with H₂-H₂O fuel.
- 2) Polarizations with CO-CO₂ tend to decrease with increasing temperature.

determined by passing a current through the battery with air at both electrodes, and their fuel cell performance has been measured with pure H₂ and with H₂-CO mixtures as fuel, and with air as the oxidant. Over twenty-four of these batteries have been tested. Their average internal resistance is 8.2 ± 1.8 ohms; and their power output, 6.7 ± 0.8 watts. Twenty of these batteries have been assembled into a system which produces over 100 watts with H₂ or H₂-CO fuel and air.

OPEN-CIRCUIT VOLTAGES

A single solid-electrolyte cell has been employed to measure the open circuit voltages developed by mixtures containing CO, H₂, CO₂, and H₂O in various amounts. This cell was fabricated by applying conventional, sintered-platinum electrodes outside and inside of the central portion of a tube of (ZrO₂)_{0.85}(CaO)_{0.15} electrolyte material as shown in Figure 1. A platinum screen was placed in the tube to serve as a current collector. A cell lead wire was attached directly to this screen. Platinum wires were wound around the electrode on the outside of the tube and could be used either as current leads or as voltage probes.

Fuel mixtures obtained by mixing varying amounts of pure hydrogen with premixed CO-CO₂ mixtures flowed inside the tubular cell, which was maintained at the desired temperature in an electrically-heated furnace. An air atmosphere surrounded the tube.

The thermodynamically predicted open-circuit voltage of the cell can be calculated by

$$E_t(4F) = RT \ln (P_{O_2,a}/P_{O_2,f}) \quad (1)$$

where 4F = 4(the Faraday number) = quantity of charge transferred per mole of O₂ passing through the electrolyte 386,000 coulombs/mole

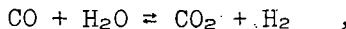
R = universal gas constant, 8.134 watt-sec./°K mole

T = absolute temperature of cell, °K

P_{O₂,a} = the partial pressure of oxygen in the air surrounding the cell, 0.21 atm.

P_{O₂,f} = the partial pressure of oxygen in the fuel gas atmosphere within the cell.

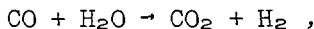
The value of P_{O₂,f} can be calculated from the composition of the fuel by standard thermodynamic methods.^{1,2} If the water gas equilibrium,



is achieved in the cell, then the fuel composition, P_{O₂,f}, and hence E_t can be determined from two parameters n₀ - the ratio of gm-atoms

- 3) The CO-CO₂ polarizations decrease with decreasing velocity of fuel flow.
- 4) Polarizations tend to increase more rapidly with current at fuel compositions where the $E_t - n\phi$ curve is sharply dropping; conversely the polarization voltage loss tends to remain more nearly constant with varying i at CO-CO₂ fuel compositions where the $E_t - n\phi$ curve is horizontal.
- 5) The αn values in the Tafel equation average about 1.0 as might be expected from simple theory which assigns α the value 0.5 and n the value 2. For the particular cell employed in this investigation the exchange current densities, i_0 , averaged about 0.7 milliamperes/cm². Insufficient data are available to draw any firm conclusions about trends of αn and i_0 with operating conditions in the cell.

The data presented in Figures 6 and 7 demonstrate that small quantities of hydrogen added to CO-CO₂ greatly reduce polarization voltage losses. With a hydrogen-carbon ratio $n_H^1 = 0.5$ the performance of the cell is essentially the same as with pure H₂. A hydrogen content of 5 mol % in a CO-H₂ mixture flowing at 1.0 cc/sec will alone support a current of 400 milliamperes; at this current the observed value of V_D from Figure 7 is about 0.15 volts if the effect of current on $n\phi$ and hence on E_t is considered. At a total current of over 1000 milliamperes (equivalent to about 40 milliamperes/cm²) the cell polarization voltage loss has risen only slightly to 0.20 volts. If the current in excess of 400 milliamperes were supported by the oxidation of CO, the data of Table 1 indicate that polarizations losses in excess of 0.30 volts could be expected at 1000 milliamperes. Apparently, the water gas shift process,



has provided sufficient hydrogen to maintain cell polarization losses low.

To investigate further the effect of hydrogen additions on the polarization losses associated with CO-CO₂ fuel mixtures - a three-cell battery, illustrated in Figures 8 and 9, was utilized. In operating on hydrogen and air this battery had higher resistance than is usually encountered in solid-electrolyte batteries of this type^{4,5} but polarization losses were negligible as shown in Figure 11. In operating on CO-CO₂ and air, however, polarizations were observed as shown in Figure 11 and in Table 2. The Tafel constants derived from the data are in good agreement with those obtained with the single cell. The difference between E_t for the CO-CO₂ fuel mixture and the observed open circuit voltage per cell in the battery is about 0.23 volts; the Tafel equation indicates that such a polarization corresponds to a current density of 6.2 milliamperes/cm²

(or 12 milliamperes/total current) passing through the cells at open circuit. This current is attributable to shunt paths in the seal regions.⁵

In a successful effort to reduce polarization losses, the CO-CO₂ fuel stream was humidified by passing it through a water bath at room temperature. At most 3 mol % H₂O was added to fuel stream. A catalyst material, Cr₂O₃, was sintered on the outside of the fuel feed tube and placed in the battery as shown in Figures 10 and 8. The performance of the battery is shown in Figure 11. (Catalyst Tubes 1 and 2 differ slightly in the quantity of Cr₂O₃ applied to the tube and the conditions of sintering.) Essentially the performance curves for the CO-CO₂ fuel mixture differ from the H₂ fuel curve only by an amount equal to three - for three cells - times the difference in E_t for the different fuels; CO-CO₂ mixtures can be utilized in solid-electrolyte cells with low polarization losses if some H₂ or H₂O is present and if a suitable shift catalyst is employed.

Additional experience on the performance of CO-H₂ fuel mixtures at higher current densities has been gained by a series of tests on a 20-cell solid-electrolyte battery whose construction and H₂-air performance have been previously described.⁵ The two H₂ performance curves of Figure 12 check with predictions based on the calculated cell resistance and on the variation of the open circuit voltage E_t with the composition of the fuel as it is gradually oxidized along the length of the battery. Polarization voltage losses are apparently negligible. The CO-H₂ performance curve was obtained without any shift catalyst present in the battery. The voltage with the CO-H₂ mixture at a current density of 450 milliamperes/cm², 0.9 ampere, is 0.1 of a volt per cell less than with pure hydrogen at the same net flow of H₂, 3 cc/sec. It can be expected that the addition of catalyst will bring about appreciable improvement of this 20-cell battery.

TWENTY-CELL BATTERIES

Twenty-five batteries identical in construction to the one whose performance is presented in Figure 12 have been fabricated and tested. All except one proved leak-tight. At the operating temperature of 1000°C battery air-air resistance - the voltage loss divided by the current value of 1.0 ampere - ranges from 6.4 to 9.4 ohms; the average and root mean-square deviation values are 7.8 ± 1.0 ohm. This average battery resistance is about 30% greater than the value calculated from the electrolyte resistivity and electrode resistance/thickness values. The open circuit voltage developed by these batteries on H₂ or H₂-CO fuel and air ranges between 19 and 20 volts; losses in the generated voltage of the solid-electrolyte bell-and-spigot cells due to shunt currents in the seal region⁵ are thus less than 7% of the reversible voltage. The maximum power output of the batteries is 6.7 ± 0.8 watts with complete combustion of H₂ fuel at about 0.87 amperes or 435 milliamperes/cm².

The resistance, open circuit voltage, and power output of these batteries are in reasonable agreement with theoretical calculations.⁵ And the methods used in fabricating the batteries yield a reasonably uniform product.

100-WATT SOLID-ELECTROLYTE FUEL-CELL POWER SUPPLY

Twenty of the 20-cell batteries described above have been used to construct a 100-watt solid-electrolyte fuel-cell power supply shown in Figure 13. The batteries are mounted on a 4.5 in. diameter metal base plate (see Figure 14) which provides support and manifolding for up to twenty-four batteries. The flow to each battery from the fuel plenum is regulated by a fine needle valve - one of which is shown on Figure 14. The valve position push rods are adjusted to equalize the flows to the batteries. The fuel flows up the feed tube to the top of the battery; it then flows downward inside the tube of cells reacting with the oxygen which passes through the electrolyte as current is drawn from the battery. The combustion products are carried down into the upper plenum of the base plate and then into the exhaust pipe.

Air surrounds the batteries inside the 3-zone furnace (see Figure 13) which is used to maintain the cells at the desired operating temperature. Plugs of insulation 5 in. in diameter and 4-1/2 in. thick are used to reduce heat losses from the top and bottom of the cylindrical heated region of the furnace. The temperature distribution throughout the batteries is indicated in Figure 15; the small circles represent individual batteries in a plan view of their arrangement in the furnace. At the top are the temperatures of the uppermost cell in three batteries indicated by Pt-Pt-10% Rh thermocouples. The middle temperatures are those on the tenth cell from the top; at the bottom are shown temperatures of the lowest cells in the batteries. With the exception of one low temperature reading on a battery opposite the "crack" of the split-tube furnace the temperatures are within $\pm 30^{\circ}\text{C}$ of the average value. Even better uniformity can be achieved by a more careful adjustment of the heat input to the various sections of the furnace.

The twenty batteries are divided into two groups of ten; in each group the batteries are electrically connected in series. The two groups, each containing 200 series-connected cells, are used in parallel to supply power to the load. The electrical performance of this power supply is shown in Figure 16. The open-circuit voltage is 200 volts; the maximum power is 102 watts at 1.2 amperes with H_2 flow at a rate corresponding to 2.1 amperes. This power output is about 20% lower than that which might be expected from the measurements of the power output of single batteries. A reduction in temperature of batteries caused by heat losses through the "split" in the furnace and a non-uniform distribution of air flow through the batteries have been shown to cause in part this reduction in power. With excess H_2 flow, the performance of the battery is improved as shown in Figure 17 and a maximum power of 110 watts is achieved.

The 100-watt power supply demonstrates the feasibility of generating fuel-cell power by means of banks of solid-electrolyte batteries. This, plus the demonstrated ability of the batteries to produce

power efficiently from carbon monoxide - carbon dioxide - water - hydrogen mixtures with the employment of a chrome oxide catalyst, demonstrates the technical feasibility of generating this power from coal.

REFERENCES

1. D. H. Archer and E. F. Sverdrup, "Solid-Electrolyte Fuel Cells" in Proceedings of the 16th Power Sources Conference, 34 (1962).
2. D. H. Archer, E. F. Sverdrup, and R. L. Zahradnik, "Coal Burning Fuel Cell Systems" Chemical Engineering Progress, 60,6, 64 (1964).
3. L. G. Austin, "Electrode Kinetics and Fuel Cells" Proceedings of the IEEE, 51, 820 (1963).
4. D. H. Archer, J. J. Alles, W. A. English, L. Elikan, E. F. Sverdrup, and R. L. Zahradnik, "Westinghouse Solid-Electrolyte Fuel Cell" in Advances in Chemistry Series (R. F. Gould, ed.), 47, 332 (1965).
5. D. H. Archer, R. L. Zahradnik, E. F. Sverdrup, W. A. English, L. Elikan, and J. J. Alles, "Solid-Electrolyte Batteries" in Proceedings of the 18th Power Sources Conference, 36 (1964).

Alcohol

Table 1

Polarization Voltage Losses, V_p , and Tafel Equation Constants at Various Fuel Flow Rates, Compositions and Temperatures

Cell Operating Conditions			Polarization Voltage Losses at Various Current Densities, volts				Tafel Constants	
% CO in CO + CO ₂ 100 (n ₀ - 1.0) ²	Temperature T, °K	Fuel Flow Q, cc/sec	i = 2 ma/cm ²	i = 4 ma/cm ²	i = 6 ma/cm ²	i = 12 ma/cm ²	cm	i ₀ , ma/cm ²
100	1215	0.7	0.19	0.27	0.30	0.39	1.1	0.33
100	1215	0.17	0.12	0.17	0.21	0.27	0.8	0.47
100	1050	0.7	0.32	0.32	0.32			
100	1050	0.17	0.19	0.20	0.21			
90	1330	0.7	0.13	0.23	0.31		1.4	0.94
25	1215	0.7	0.11	0.175	0.22		0.9	0.64
25	1215	0.17	0.065	0.14	0.195		1.1	1.20
25	1050	0.7	0.29	0.375				
25	1050	0.17	0.28	0.34				
10	1215	0.7	0.09	0.16	0.19	0.24	0.8	0.80
10	1215	0.17	0.09	0.11				
10	1050	0.7	0.275	0.34				
10	1050	0.17	0.235	0.255				

Table 2

Polarization Voltage Losses with CO-CO₂ in a Three-Cell Solid-Electrolyte Battery

Fuel: 90 mol % CO, 10 mol % CO₂
 $n' = 1.1$
 5.7 cc/sec
 Oxidant: air
 Temperature: 1000°C
 Cell area (active): 2.0 cm²

Current density, $I/A_p = 1$, milliamperes/cm ² :	25	50	100	150
Polarization Voltage loss, V_p , volts:	0.37	0.44	0.51	0.55

Derived Tafel constants: $\alpha_n = 0.92$
 $i_0 = 0.6$ milliamperes/cm²

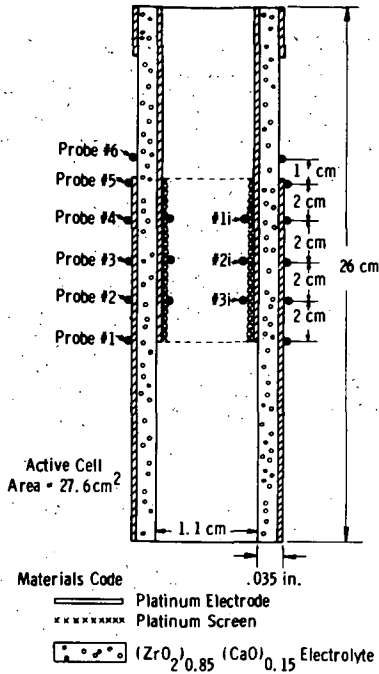


Fig. 1—Schematic cross section of fuel cell TC#8

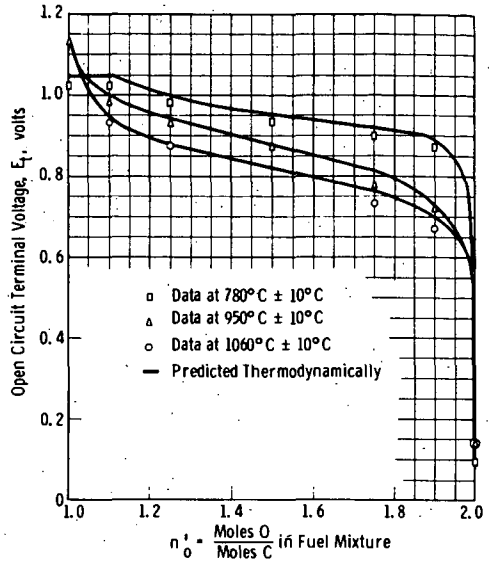


Fig. 2—Generated voltage of a fuel cell using a C-O fuel mixture as a function of fuel mixture composition

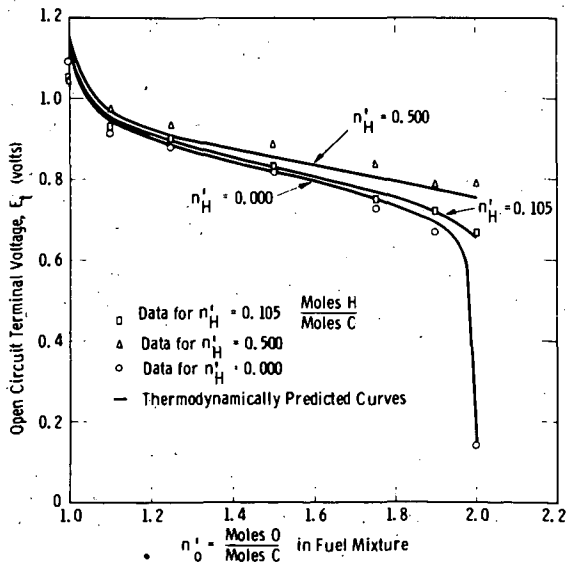


Fig. 3—Generated voltage of a fuel cell using a C-H-O fuel mixture at 1060°C as a function of fuel mixture composition

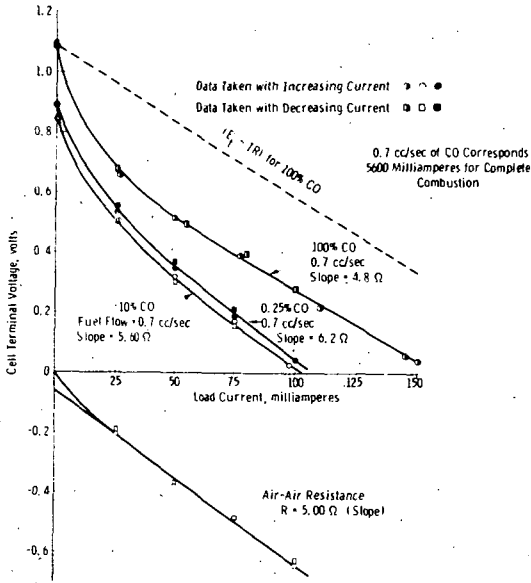


Fig. 4 - Load curves for fuel cell TC #8 using CO-CO₂ fuel mixtures at 780°C

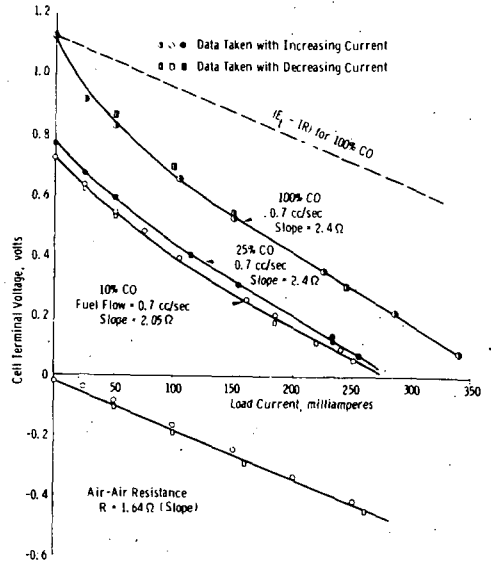


Fig. 5 - Load curves for fuel cell TC #8 using CO-CO₂ fuel mixtures at 940°C

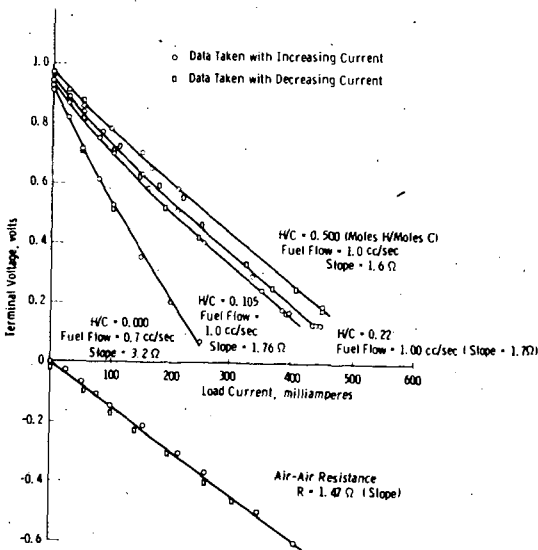


Fig. 6 - Load curves for fuel cell TC #8 using C-H-O fuel mixtures at 1060°C with $n^+ = 1.10$ (Moles O/Moles C) in fuel chamber

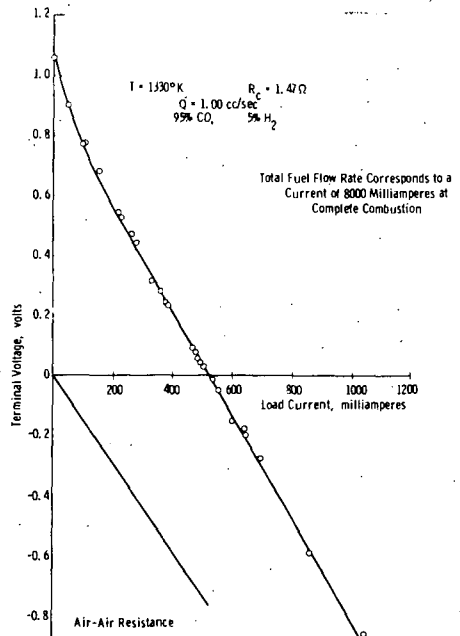


Fig. 7 - Load curve demonstrating effectiveness of water-gas reaction in improving fuel cell performance in TC #8

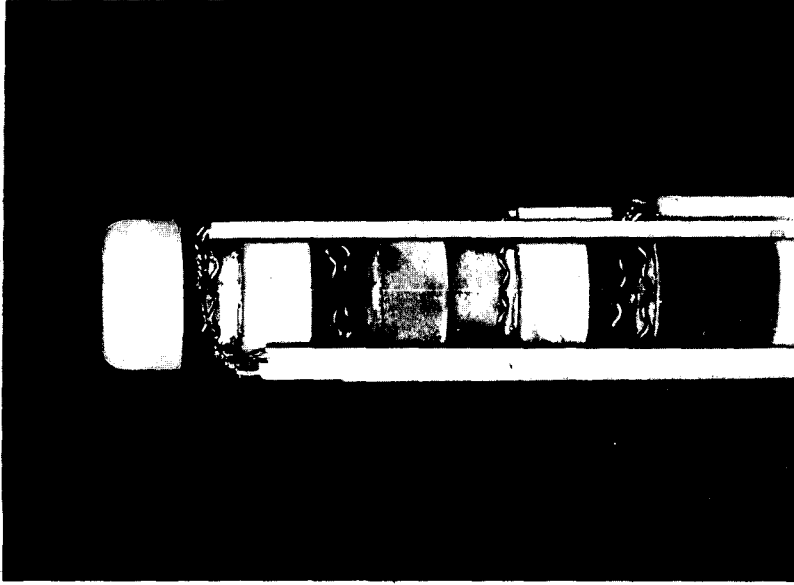


Fig. 9—Three-cell solid-electrolyte battery with current leads, voltage taps, and thermocouple probes

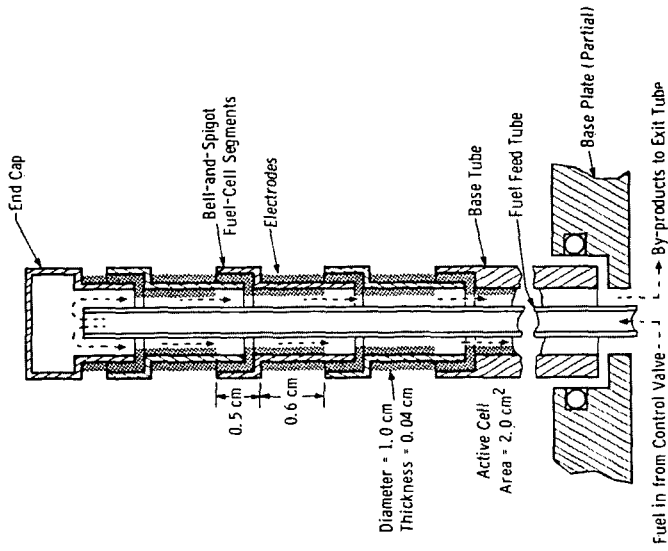


Fig. 8—Schematic axial cross-section of a three-cell solid electrolyte battery showing feed-tube

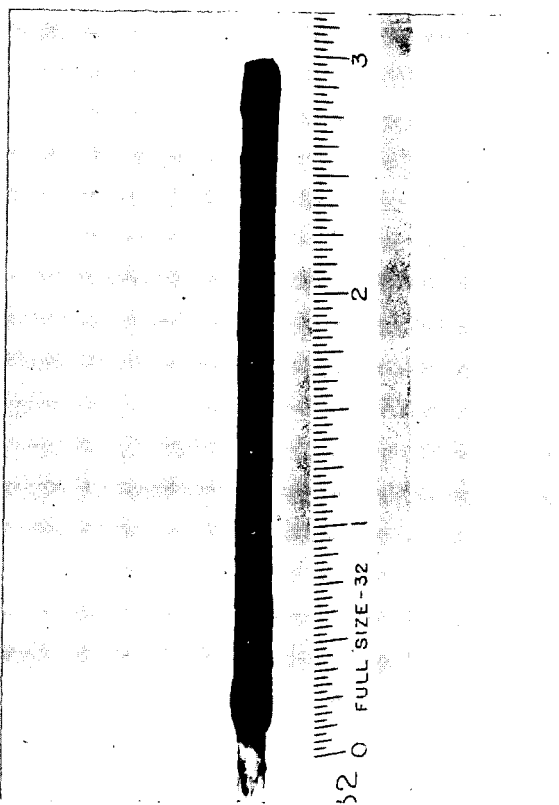


Fig. 10—Fuel feed tube for three-cell battery with Cr_2O_3 catalyst coating

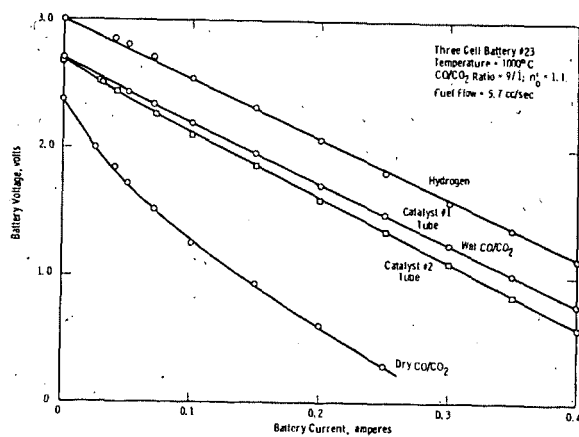


Fig. 11—Performance of three cell battery using chrome-oxide catalyst sintered to fuel feed tube

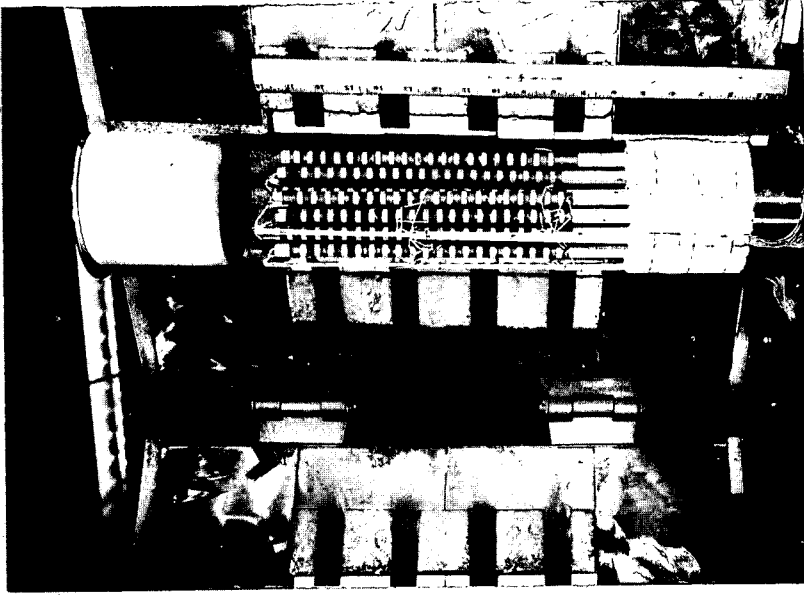


Fig. 13—100-watt solid-electrolyte fuel-cell power generator with furnace door open

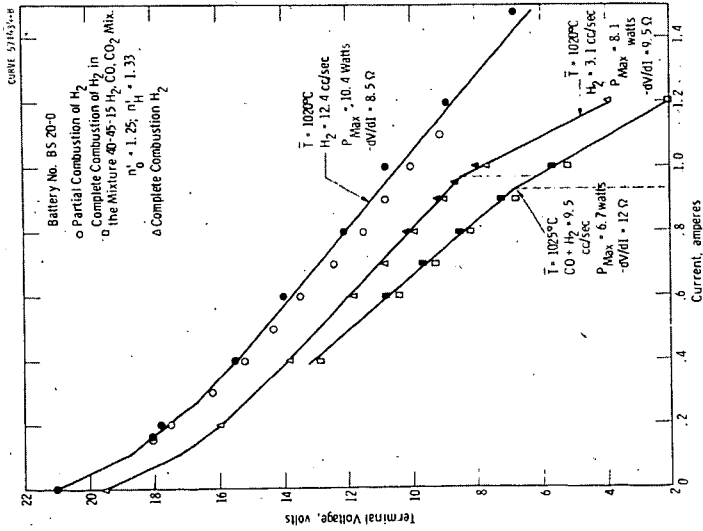


Fig. 12—Twenty-cell solid-electrolyte battery performance

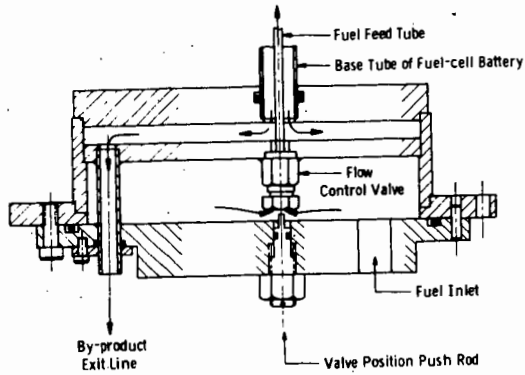


Fig. 14 - Section view of base plate

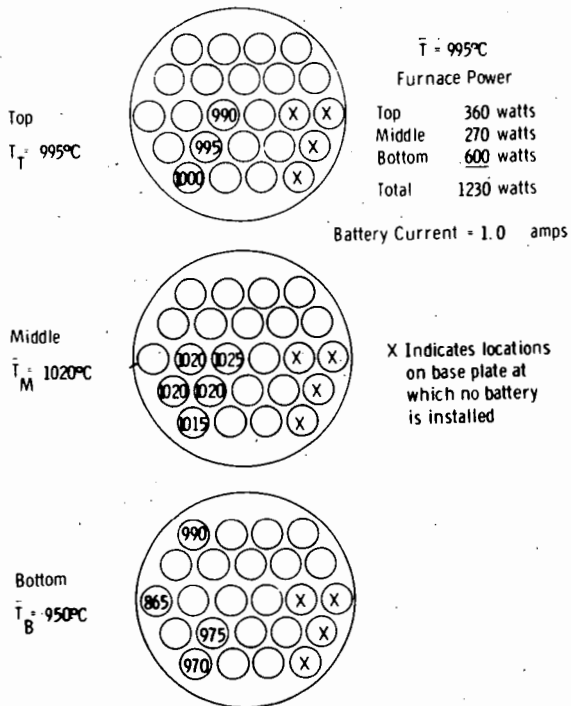


Fig. 15 - Battery temperature distribution as a function of axial position --at operating temperature

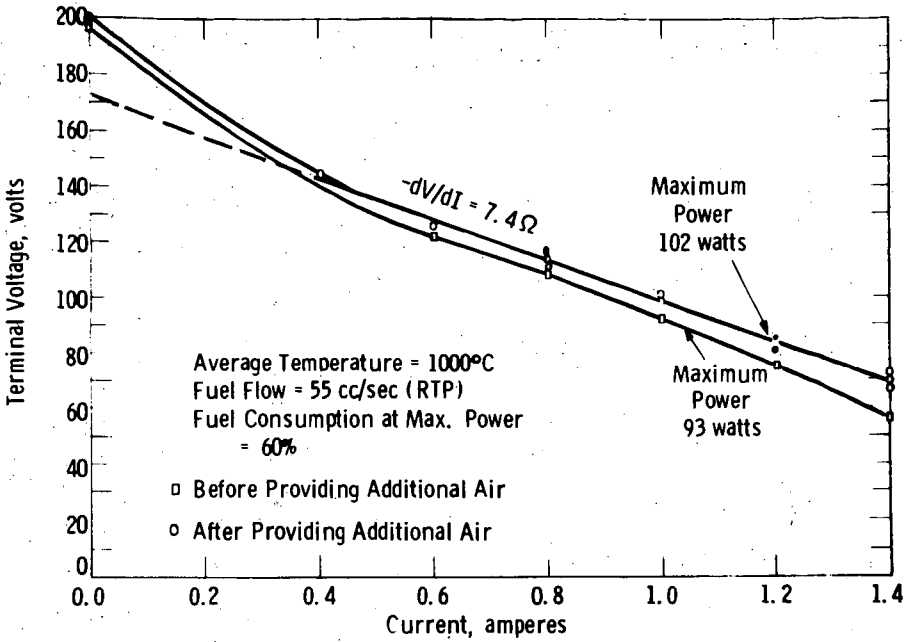


Fig. 16—100-watt battery performance before and after increasing air flow

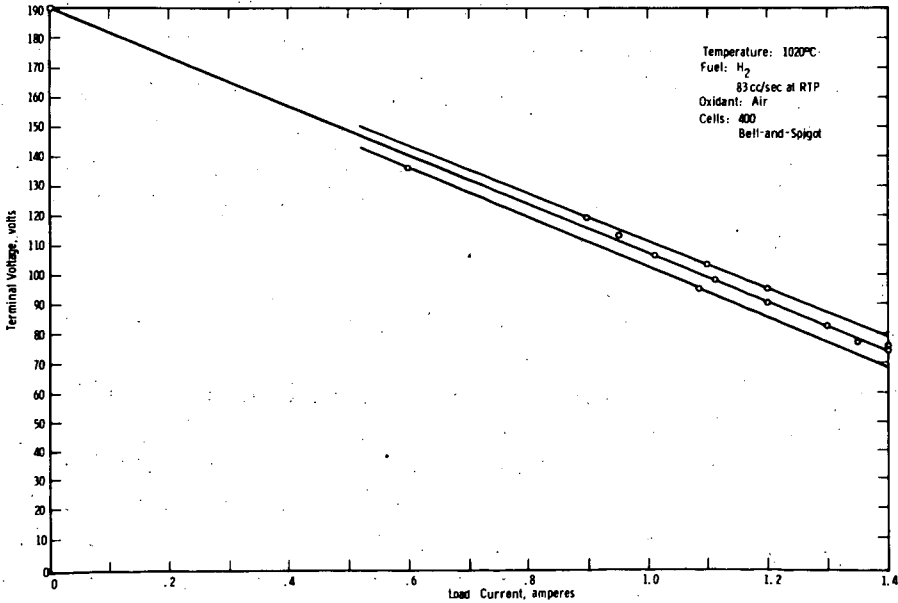


Fig. 17—Performance of 100-watt solid-electrolyte fuel-cell power system